

Percolation assisted excitation transport in discrete-time quantum walks

M. Štefaňák, J. Novotný and I. Jex

Department of Physics, Faculty of Nuclear Sciences and Physical Engineering, Czech Technical University in Prague, Břehová 7, 115 19 Praha 1 - Staré Město, Czech Republic

Abstract. Coherent transport of excitations along chains of coupled quantum systems represents an interesting problem with a number of applications ranging from quantum optics to solar cell technology. A convenient tool for studying such processes are quantum walks. They allow to determine in a quantitative way all the process features. We study the survival probability and the transport efficiency on a simple, highly symmetric graph represented by a ring. The propagation of excitation is modeled by a discrete-time (coined) quantum walk. For a two-state quantum walk, where the excitation (walker) has to leave its actual position to the neighboring sites, the survival probability decays exponentially and the transport efficiency is unity. The decay rate of the survival probability can be estimated using the leading eigenvalue of the evolution operator. However, if the excitation is allowed to stay at its present position, i.e. the propagation is modeled by a lazy quantum walk, then part of the wave-packet can be trapped in the vicinity of the origin and never reaches the sink. In such a case, the survival probability does not vanish and the excitation transport is not efficient. The dependency of the transport efficiency on the initial state is determined. Nevertheless, we show that for some lazy quantum walks dynamical percolations of the ring eliminate the trapping effect and efficient excitation transport can be achieved.

1. Introduction

Quantum walks [1, 2, 3] emerged as an extension of the concept of a classical random walk to the evolution of a quantum particle on a graph or lattice. They were applied to various problems of quantum information, such as quantum search of an unsorted database [4, 5, 6, 7, 8], perfect state transfer [9, 10, 11, 12, 13], graph isomorphism testing [14, 15, 16] or finding structural anomalies in graphs [17, 18, 19]. Moreover, quantum walks were shown to be universal tools for quantum computation [20, 21]. Up to date quantum walks were realized in a number of experiments utilizing optically trapped atoms [22], cold ions [23, 24] and photons [25, 26, 27, 28, 29, 30, 31]. Recently, an experimental realization of quantum walk on dynamically percolated line was performed [32].

Quantum walks have been also intensively studied in the context of coherent transport on graphs or networks of coupled quantum systems. Among the first studies the Hadamard walk on a half-line with one absorbing boundary (sink) was analyzed in [33]. The authors have found that the particle has a non-zero chance to escape to infinity, in contrast to the classical result where the particle falls into the sink with certainty. This problem was later studied in a number of alternated configurations, coins a geometries [34, 35, 36, 37, 38, 39]. Dependence of the absorption probability on the initial condition for quantum walk on finite line with two sinks was analyzed in [34]. The time dependence of the absorption probability was studied in [35] for quantum walk on a line with one and two sinks. The authors have also proposed an extension to d -dimensional walk with $d - 1$ -dimensional absorbing wall. The paper [36] analyzed the absorbing times for quantum walks on hypercube. In [37] the authors have considered quantum walk on a line with one or two moving sinks. More recently, enhancement of transport by noise in quantum walk on a closed loop was identified in [38]. In [39] the authors have found edge-state enhanced transport along the cut between the source and the absorption center in a two-dimensional quantum walk. For continuous-time quantum walks the effects of trapping, scaling and percolation on transport have been discussed in [51, 52, 53, 54].

Discrete time quantum walks represent nontrivial dynamics of two degrees of freedom given by the coin and the position. Due to this they offer a formidable playground to test the influence of noise, external perturbations or loss of control over the system representing all possible aspects of open system dynamics. By considering walks on changing graph structure a natural link to percolation theory was established and it is of interest to study alternation of transport efficiency due to percolation.

We carry out one of the simplest nontrivial percolation assisted transports. Under transport we understand the gradual leak of the initially localized excitation at a preassigned position called sink. In the present paper we study the transport of the excitation to the sink on a ring graph. The ring graph was chosen as it is highly symmetric and for even number of sites we can study the transport across the structure through two equal segments assuming we choose as source and drain two opposite

positions. The ring structure – due to its high symmetry – allows to study the ideal (non-percolated) dynamics for a large class of quantum walks in a closed form and identify the effect of percolation in quite a transparent way.

We focus on two different scenarios. Namely, the propagation of excitation is described either by a two-state or a three-state (lazy) discrete-time quantum walk. The two-state walk model where the excitation has to leave its present position was to some extent analyzed in [34, 35]. The excitation is fully transferred to the sink independent of the initial conditions. The rate of the transport depends on the size of the ring and the coin operator which determines the spreading of the excitation’s wave-packet. This case will serve as the reference for the more involved lazy walk. When we consider the transport described by a lazy quantum walk where the particle is allowed to stay at its actual position, the situation becomes more interesting. Indeed, certain lazy quantum walks are able to trap part of the wave-function in the vicinity of the origin [40, 41], i.e. the probability of finding the excitation at finite positions does not vanish in the limit of infinite number of steps. This feature crucially depends on the choice of the coin operator [42, 43]. The consequence of the trapping effect is that the transport of excitation in the lazy quantum walk is not fully efficient. Nevertheless, we show that dynamical percolations [44, 45] of the ring can eliminate the trapping effect and improve the transport efficiency.

The paper is organized as follows: In Section 2 we describe the model of excitation transport based on a discrete-time quantum walk. The two-state walk model is analyzed in Section 3. Section 4 is devoted to the lazy walk model. The effect of dynamical percolations on the transport efficiency is discussed in Section 5. We conclude and present an outlook in Section 6. More technical details of calculating the survival probability for a two-state walk are left for Appendix A.

2. Transport of excitation in discrete-time quantum walk

In this Section we formally describe our model. We consider the transport of excitation to the sink on a finite-size ring described by a discrete-time quantum walk. The vertices of the ring have labels from $-N + 1$ to N . The sink, which takes the excitation away from the ring, is located at the vertex N . Note that this configuration is equivalent to a finite line from $-N$ to N with sinks at both ends. The Hilbert space of the quantum walk has the tensor product structure

$$\mathcal{H} = \mathcal{H}_P \otimes \mathcal{H}_C,$$

where \mathcal{H}_P is the position space spanned by the vectors $|m\rangle$, with $m = -N + 1, \dots, N$, corresponding to the excitation being at the vertex m . By \mathcal{H}_C we denote the coin space which describes the internal degree of freedom of the excitation. The excitation enters the ring exactly opposite the sink with some coin state $|\psi_C\rangle \in \mathcal{H}_C$, i.e. the initial state is

$$|\psi_{in}\rangle = |0\rangle|\psi_C\rangle.$$

A single time-step consists of a quantum walk evolution \hat{U}

$$\hat{U} = \hat{S} \cdot (\hat{I}_P \otimes \hat{C}),$$

where the step operator \hat{S} and the coin operator \hat{C} will be specified later. This is followed by a projection

$$\hat{\pi} = \left(\hat{I}_P - |N\rangle\langle N| \right) \otimes \hat{I}_C,$$

corresponding to the effect of the sink. Hence, the complete time evolution is not unitary and the state of the excitation after t steps is described by vector

$$|\psi(t)\rangle = \left(\hat{\pi} \cdot \hat{U} \right)^t |\psi_{in}\rangle,$$

with norm generally less than unity.

In the following we analyze the properties of the survival probability $\mathcal{P}(t)$, i.e. the probability that the excitation remains on the ring until time t , which is given by

$$\mathcal{P}(t) = \langle \psi(t) | \psi(t) \rangle,$$

and the asymptotic transport efficiency η which we define as

$$\eta = 1 - \lim_{t \rightarrow \infty} \mathcal{P}(t).$$

In Section 3 we consider the two-state quantum walk model, while in Section 4 we focus on the lazy model. Before we turn to these models we first derive an asymptotic estimate of the survival probability $\mathcal{P}(t)$. We begin with the estimate

$$\mathcal{P}(t) \leq \left\| \left(\hat{\pi} \cdot \hat{U} \right)^t \right\|^2 = \exp \left(2t \ln \left(\left\| \left(\hat{\pi} \cdot \hat{U} \right)^t \right\|^{\frac{1}{t}} \right) \right).$$

For large t the argument of the logarithm can be estimated according to

$$\left\| \left(\hat{\pi} \cdot \hat{U} \right)^t \right\|^{\frac{1}{t}} \approx |\lambda_l|,$$

where λ_l is the leading eigenvalue of $\hat{\pi} \cdot \hat{U}$, i.e. the largest eigenvalue in absolute value. When $|\lambda_l|$ is close to unity (but less than one) we make the first-order Taylor expansion of the logarithm

$$\ln \left(\left\| \left(\hat{\pi} \cdot \hat{U} \right)^t \right\|^{\frac{1}{t}} \right) \approx \ln |\lambda_l| \approx -(1 - |\lambda_l|).$$

Hence, when the absolute value of the leading eigenvalue λ_l of $\hat{\pi} \cdot \hat{U}$ is smaller than one we find that the survival probability behaves in the asymptotic limit as an exponential

$$\mathcal{P}(t) \sim e^{-\gamma t}, \tag{1}$$

where the decay rate γ reads

$$\gamma = 2(1 - |\lambda_l|). \tag{2}$$

In such a case, the asymptotic transport efficiency η is unity. However, when $|\lambda_l| = 1$ the survival probability does not vanish and the transport is not efficient. We will see in Section 4 that such situation occurs in certain lazy quantum walks.

3. Two-state walk model

Let us begin with the two-state walk model, i.e. the particle has to move in each time step from the vertex m to the nearest neighbours $m - 1$ or $m + 1$. The coin space \mathcal{H}_C is two-dimensional, we denote the basis vectors corresponding to the steps to the left and right as $|L\rangle$ and $|R\rangle$. The step operator of the two-state quantum walk is then given by

$$\hat{S}^{(2)} = \sum_{m=-N+1}^N |m-1\rangle\langle m| \otimes |L\rangle\langle L| + |m+1\rangle\langle m| \otimes |R\rangle\langle R|, \quad (3)$$

where we consider periodic boundary condition $N \equiv -N$. As for the coin operator \hat{C} , for simplicity we consider a one-parameter family which is in the standard basis of the coin space given by the matrix

$$C^{(2)} = \begin{pmatrix} \rho & \sqrt{1-\rho^2} \\ \sqrt{1-\rho^2} & -\rho \end{pmatrix}, \quad \rho \in (0, 1). \quad (4)$$

Nevertheless, this choice in fact covers all $U(2)$ matrices due to unitary equivalence which was recently found in [46]. The coin parameter ρ determines the rate at which the excitation spreads through the ring [47]. The choice of $\rho = \frac{1}{\sqrt{2}}$ corresponds to the familiar and extensively studied case of the Hadamard walk.

In Figure 1 we present the numerical simulation of the survival probability $\mathcal{P}(t)$ for the Hadamard walk ($\rho = \frac{1}{\sqrt{2}}$) on the ring consisting of 10 vertices, i.e. $N = 5$. The left plot shows the survival probability for the first 100 steps. Due to the symmetries of the model we consider, i.e. the excitation enters the ring exactly opposite the sink, the survival probability is exactly the same for all initial coin states $|\psi_C\rangle$. This follows from the results of [34], as we show in Appendix A. The right plot displays the survival probability on a longer time scale of 1000 steps. To unravel the asymptotic behavior of $\mathcal{P}(t)$ we use logarithmic scale on the y axis. The plot indicates that the survival probability decays exponentially (1) with the decay rate (2) determined by the leading eigenvalue of $\hat{\pi} \cdot \hat{U}$.

The decay rate γ depends crucially both on the coin parameter ρ and the size of the ring N . We plot the decay rate γ as a function of the coin parameter ρ in Figure 2. For ρ approaching zero the decay rate vanishes. Indeed, for $\rho = 0$ the coin operator (4) turns into a permutation matrix. In such a case, the excitation never leaves the vertices $-1, 0$ and 1 , i.e. it never reaches the sink and the asymptotic transport efficiency η is zero, except for $N = 1$ when the ring consists only of the source and the sink. On the other hand, for ρ approaching unity the decay rate increases rapidly. In the limiting case of $\rho = 1$ the coin operator (4) reduces to an identity with an additional phase shift of π on the $|R\rangle$ state. Hence, the excitation is fully transported into the sink after N steps and the survival probability is a step function, with $\mathcal{P}(t) = 1$ for $t < N$ and $\mathcal{P}(t) = 0$ for $t \geq N$.

In Figure 3 we consider the decay rate γ as a function of the size of the ring N . For the plot on the left we have chosen the coin parameter $\rho = \frac{1}{\sqrt{2}}$ corresponding to the

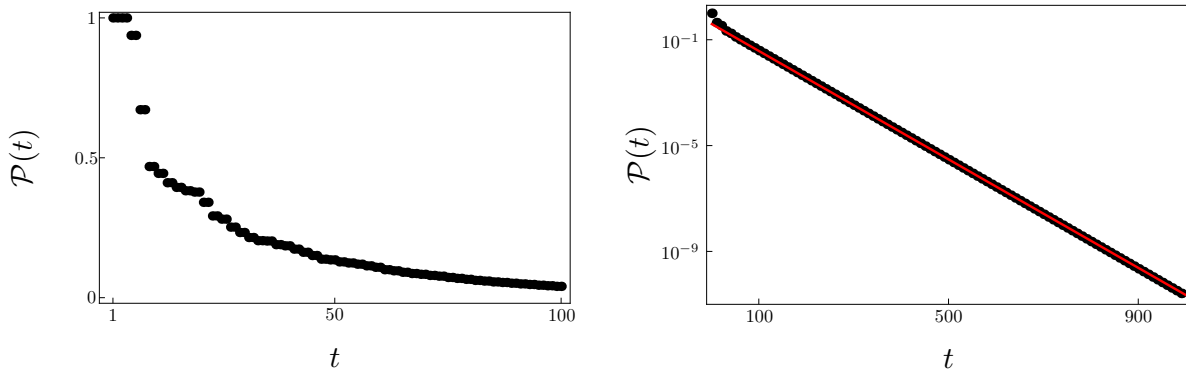


Figure 1. On the left we display the survival probability $\mathcal{P}(t)$ for the Hadamard walk (i.e. $\rho = \frac{1}{\sqrt{2}}$). Due to the symmetries of the model the survival probability $\mathcal{P}(t)$ is independent of the initial coin state. On the right we show the asymptotic behavior of the survival probability $\mathcal{P}(t)$ for the Hadamard walk. The log-scale reveals that the survival probability decays exponentially. The red curve is given by (1). The size of the ring is given by $N = 5$, i.e. 10 vertices.

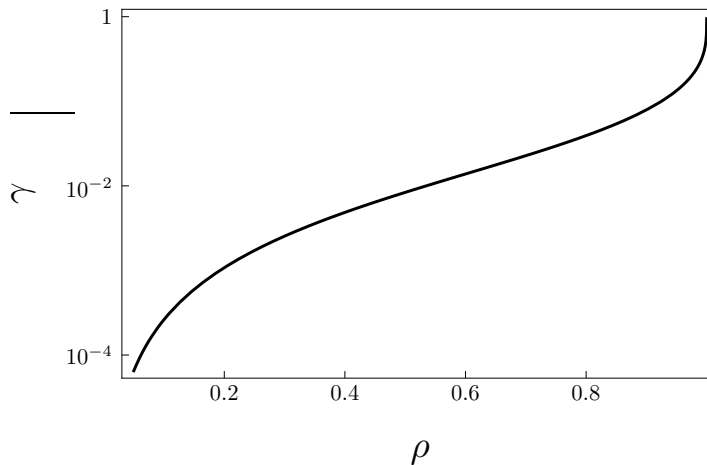


Figure 2. The decay rate γ as a function of the coin parameter ρ . The size of the ring is given by $N = 5$.

Hadamard walk, while in the right plot we have considered $\rho = 0.8$. The log-log scale reveals that the decay rate obeys a power law

$$\gamma \sim N^{-3}, \quad (5)$$

independent of the coin parameter ρ .

We point out that for large N the decay rate γ is very small. Hence, it takes a considerable number of steps for the exponential behaviour of the survival probability (1) to set in. As was established and explained at length in Section 4.6 of [35], repeated reflections from the sink (or, in fact, from the adjacent points) slow the decay of the survival probability in the intermediate regime to a power law

$$\mathcal{P}(t) \sim t^{-\frac{1}{2}}. \quad (6)$$

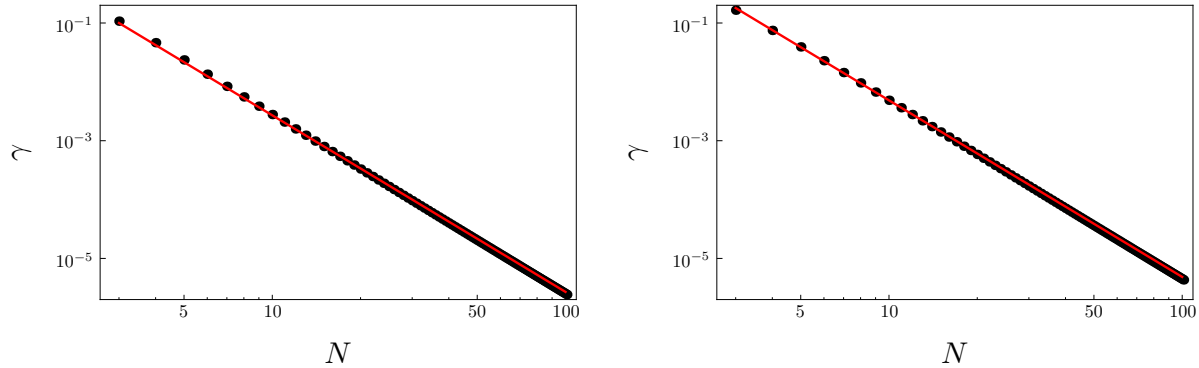


Figure 3. The decay rate γ as a function of the size of the ring N . Left plot shows the choice $\rho = \frac{1}{\sqrt{2}}$ corresponding to the Hadamard walk, while in the right plot we have chosen $\rho = 0.8$. The plots indicate that the decay rate obeys a power law (5). This behaviour is independent of the coin parameter ρ .

Nevertheless, after an order of N^3 steps the survival probability begins to deviate from the power law (6) and tends to follow the exponential dependence on the number of steps (2). We illustrate this property in Figure 4.

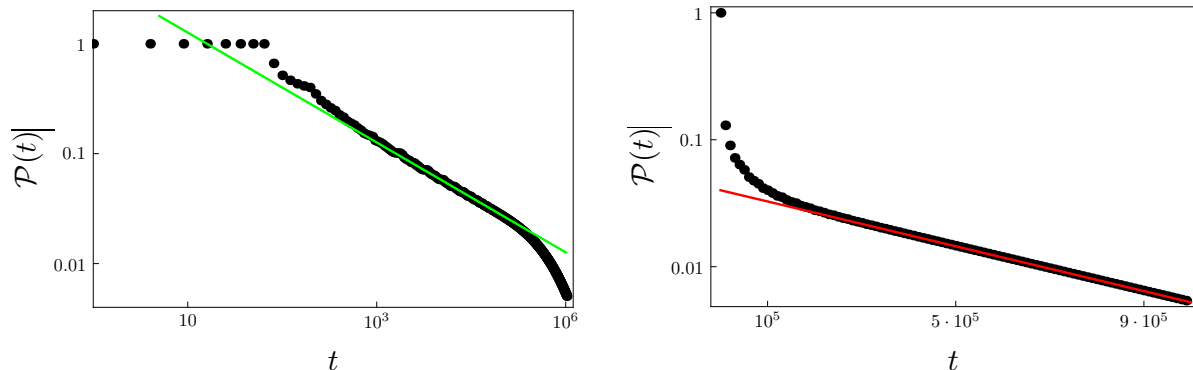


Figure 4. Survival probability for the Hadamard walk on a ring with 100 vertices, i.e. $N = 50$. On the left we display $\mathcal{P}(t)$ on a log-log scale. The green line corresponds to the power law behavior of (6). We observe that it fits well in the intermediate regime, however, it deviates on the long time scale. Indeed, the plot on the right, where we display the survival probability on a log-scale, shows that in the asymptotic regime the behavior of $\mathcal{P}(t)$ follows the exponential (1) depicted by the red line.

To summarize this section, for the two-state model the survival probability $\mathcal{P}(t)$ is independent of the initial coin state and decays exponentially. Hence, the asymptotic transport efficiency η is unity.

4. Lazy walk model

We now turn to the lazy walk model. Let us denote the basis coin states corresponding to the step to the left, stay, and the step to the right as $|L\rangle$, $|S\rangle$ and $|R\rangle$. The step

operator of a lazy quantum walk on a ring is then given by the following extension of the step operator for a two-state walk (3)

$$\hat{S}^{(3)} = \hat{S}^{(2)} + \sum_{m=-N+1}^N |m\rangle\langle m| \otimes |S\rangle\langle S|.$$

Next, we choose the coin operator which exhibits the trapping effect. The complete set of such coins for a lazy walk was determined in [43]. For simplicity, we consider a two-parameter set of coins which are in the standard basis of the coin space $\{|L\rangle, |S\rangle, |R\rangle\}$ given by the matrix

$$C^{(3)} = \begin{pmatrix} -\rho^2 & \rho\sqrt{2-2\rho^2} & e^{-i\alpha}(1-\rho^2) \\ \rho\sqrt{2-2\rho^2} & 2\rho^2-1 & e^{-i\alpha}\rho\sqrt{2-2\rho^2} \\ e^{i\alpha}(1-\rho^2) & e^{i\alpha}\rho\sqrt{2-2\rho^2} & -\rho^2 \end{pmatrix} \quad (7)$$

where ρ ranges from zero to one and the phase α from 0 to 2π . The parameter ρ has the same interpretation as for the two-state walk of Section 3. The phase α will not play a role in this Section, however, it will be crucial when we consider percolations in Section 5.

The trapping effect arises when the evolution operator of the quantum walk has a highly degenerate eigenvalue and the corresponding eigenstates are spatially localized [40, 41]. One can show by direct calculation that this is the case for the lazy walk on ring with the coin (7). Indeed, the evolution operator \hat{U} has an eigenvalue $\lambda = 1$ with $2N$ -fold degeneracy and the corresponding eigenvectors (linearly independent but overlapping) read

$$\begin{aligned} |s_n\rangle = & |n\rangle \left(\sqrt{1-\rho^2}|L\rangle + \frac{\rho}{\sqrt{2}}|S\rangle \right) + \\ & + |n+1\rangle \left(\frac{\rho}{\sqrt{2}}|S\rangle + e^{i\alpha}\sqrt{1-\rho^2}|R\rangle \right), \end{aligned} \quad (8)$$

where n ranges from $-N+1$ to N . Notice that only two of these vectors, namely $|s_{N-1}\rangle$ and $|s_N\rangle$, have support on the vertex N where the sink is located. Hence, the vectors $|s_n\rangle$ with $n \in \{-N+1, \dots, N-2\}$ are not affected by the sink and they are eigenvectors of $\hat{\pi} \cdot \hat{U}$ with eigenvalue one. Consequently, the trapping effect remains even in the presence of the sink, the survival probability has a non-vanishing limit and the excitation transport is not fully efficient.

Let us now evaluate the transport efficiency η . Using the Gram-Schmidt procedure one can form an orthonormal basis in the degenerate subspace from the eigenstates (8). We denote the basis vectors by $|\phi_n\rangle$. The probability of trapping the excitation on the vertex m , i.e. the probability of finding the excitation at position m in the limit of infinite number of steps, is obtained from

$$p_T(m) = \sum_{i=L,S,R} \left| \langle m|i| \left(\sum_n |\phi_n\rangle\langle\phi_n| \right) |\psi_{in}\rangle \right|^2. \quad (9)$$

The limiting value of the survival probability is then given by summing the trapping probabilities over all vertices of the ring excluding the sink

$$\lim_{t \rightarrow \infty} \mathcal{P}(t) = \sum_{m=-N+1}^{N-1} p_T(m),$$

which can be simplified into

$$\lim_{t \rightarrow \infty} \mathcal{P}(t) = \sum_{n=-N+1}^{N-2} |\langle \psi_{in} | \phi_n \rangle|^2.$$

Hence, the asymptotic transport efficiency reads

$$\eta = 1 - \sum_{n=-N+1}^{N-2} |\langle \psi_{in} | \phi_n \rangle|^2.$$

The evaluation of η is readily done for small N . We present the results for $N = 2, \dots, 5$ in Table 1.

N	η
2	$1 - \frac{2(1-\rho^2)}{4-3\rho^2} h_2 ^2 - \frac{2}{4-\rho^2} h_+ ^2$
3	$1 - 4(2 - \rho^2) \left(\frac{(1-\rho^2) h_2 ^2}{16-20\rho^2+5\rho^4} + \frac{ h_+ ^2}{16-12\rho^2+\rho^4} \right)$
4	$1 - 2(16 - 16\rho^2 + 3\rho^4) \left(\frac{(1-\rho^2) h_2 ^2}{64-7\rho^2(\rho^2-4)^2} + \frac{ h_+ ^2}{64-\rho^2(\rho^4-24\rho^2+80)} \right)$
5	$1 - 8(2 - \rho^2)(\rho^4 - 8\rho^2 + 8) \left(\frac{(1-\rho^2) h_2 ^2}{(3\rho^2-4)(3\rho^6-36\rho^4+96\rho^2-64)} + \frac{ h_+ ^2}{\rho^8-40\rho^6+240\rho^4-448\rho^2+256} \right)$

Table 1. Asymptotic transport efficiency η for small rings up to $N = 5$.

In order to reduce the complexity of the formulas we have expressed the initial coin state $|\psi_C\rangle$ in terms of a more suitable basis of the coin space. Following [48] we have chosen the basis formed by the eigenvectors of the coin operator (7)

$$\begin{aligned} |\sigma^+\rangle &= \sqrt{\frac{1-\rho^2}{2}} |L\rangle + \rho |S\rangle + \sqrt{\frac{1-\rho^2}{2}} e^{i\alpha} |R\rangle, \\ |\sigma_1^-\rangle &= \frac{\rho}{\sqrt{2}} |L\rangle - \sqrt{1-\rho^2} |S\rangle + \frac{\rho}{\sqrt{2}} e^{i\alpha} |R\rangle, \\ |\sigma_2^-\rangle &= \frac{1}{\sqrt{2}} (|L\rangle - e^{i\alpha} |R\rangle). \end{aligned} \tag{10}$$

The initial coin state is in the eigenbasis decomposed according to

$$|\psi_C\rangle = h_+|\sigma^+\rangle + h_1|\sigma_1^-\rangle + h_2|\sigma_2^-\rangle.$$

There are several advantages of using the basis (10). First, η is independent of the amplitude h_1 , as can be seen from Table 1. Indeed, for $h_1 = 1$ and $h_+ = h_2 = 0$ the trapping effect vanishes [48]. Hence, the initial coin state $|\sigma_1^-\rangle$ is the only one for which the transport efficiency η is unity. Next, η does not depend on the phase α which was absorbed into the definition of the eigenbasis (10). Thus, the coins with different values of α are equivalent \ddagger . Finally, the amplitudes h_+ and h_2 enter the formula for the transport efficiency η only as probabilities $|h_+|^2$ and $|h_2|^2$ of finding the particle initially in the coin state $|\sigma^+\rangle$ or $|\sigma_2^-\rangle$. Hence, the efficiency of transfer is given by incoherent contributions from the two relevant basis states. It is then straightforward to show that the worst transport efficiency arises when the initial coin state is chosen as $|\sigma^+\rangle$.

To illustrate our results we display in Figure 5 the survival probability for the Grover walk (i.e. $\rho = \frac{1}{\sqrt{3}}$ and $\alpha = 0$), when the initial coin state is chosen as $|\sigma_1^-\rangle$ (left plot) or $|\sigma^+\rangle$ (right plot). For $|\sigma_1^-\rangle$ the trapping effect disappears and the survival probability decays exponentially (1), similarly to the two-state walk of Section 3. The decay rate γ can be estimated using the sub-leading eigenvalue λ_{sl} of $\hat{\pi} \cdot \hat{U}$ according to

$$\gamma = 2(1 - |\lambda_{sl}|). \quad (11)$$

Nevertheless, for all other initial coin states the trapping effect results in non-vanishing limit of the survival probability. For $|\sigma^+\rangle$ the trapping effect is the strongest. The right plot indicates that the survival probability does not drop below the value

$$\sum_{m=-N+1}^{N-1} p_T(m) \approx 0.55, \text{ which is depicted by the red line.}$$

For larger rings the Gram-Schmidt procedure becomes tedious and, moreover, the resulting formula for the transport efficiency η is rather lengthy. Nevertheless, we can estimate the transport efficiency following the analysis of the walk on an infinite line. We approximate the trapping probability at position m (9) using the results obtained for infinite line in [48] where it was found

$$p_T(m) = \begin{cases} \frac{2-2\rho^2}{\rho^4} Q^{2m} |h_+ + h_2|^2, & m > 0, \\ \frac{Q}{\rho^2} \{|h_+|^2 + (1 - \rho^2)|h_2|^2\}, & m = 0. \\ \frac{2-2\rho^2}{\rho^4} Q^{2|m|} |h_+ - h_2|^2, & m < 0 \end{cases} \quad (12)$$

Here the quotient Q reads

$$Q = \frac{2 - \rho^2 - 2\sqrt{1 - \rho^2}}{\rho^2}.$$

\ddagger This is no longer true when we consider percolations of the ring, as we will show in the following Section.

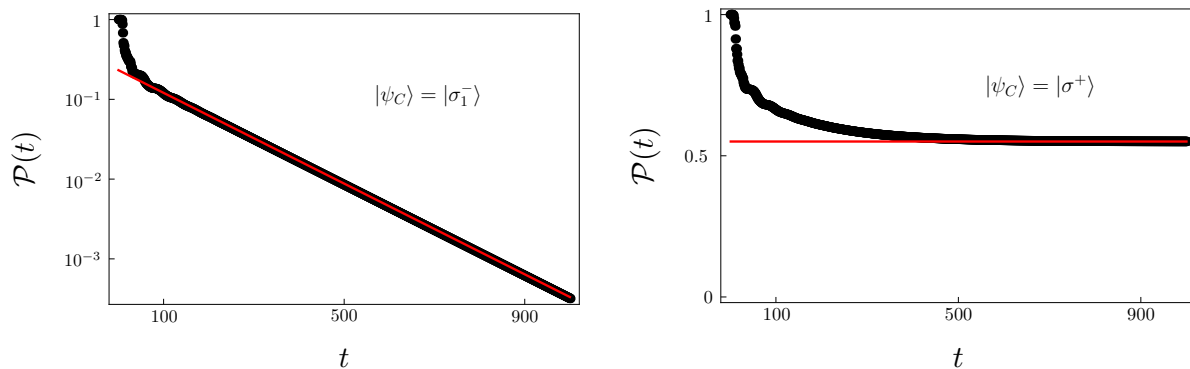


Figure 5. Survival probability for the Grover walk on a ring with 10 vertices, i.e. $N = 5$ in dependence on the number of steps. On the left we have chosen the initial coin state as $|\sigma_1^-\rangle$ for which the trapping effect disappears. In such a case the survival probability $\mathcal{P}(t)$ vanishes exponentially. This is highlighted by the log-scale. The red line corresponds to the decay rate γ determined by (11). The right plot shows the survival probability when the initial coin state is $|\sigma^+\rangle$ for which the trapping effect is the strongest. The survival probability approaches the red line given by $\sum_{m=-N+1}^{N-1} p_T(m) \approx 0.55$.

Hence, the asymptotic transport efficiency for a ring of size $2N$ can be estimated by

$$\eta \approx 1 - \frac{Q}{\rho^2} \left(\sqrt{1 - \rho^2} (1 - Q^{2(N-1)}) (|h_2|^2 + |h_+|^2) + (1 - \rho^2) |h_2|^2 + |h_+|^2 \right).$$

Since the trapping probability (12) decays very fast (exponentially) with the distance from the origin, this approximation is quite good even for small rings. The difference is most profound for the coin parameter ρ close to one. With increasing size of the ring the differences become negligible. This result also confirms that the worst transport efficiency is obtained for the initial coin state $|\sigma^+\rangle$.

5. Dynamical percolation of the ring

In this Section we analyze the effect of dynamical percolation of the ring on the transport efficiency of the lazy quantum walk. Percolation can be viewed as a special (but realistic) noise source and hence the problem at hand can be cast under the headline of noise assisted excitation transfer. Improving transport by allowing the edges to break randomly seems to be a bit counterintuitive at the first sight. However, percolations can in some situations eliminate the localized eigenstates (8) and thus improve the asymptotic transport efficiency to unity.

The evolution of the percolated quantum walk can be described within the framework of random unitary channels [49, 50]. The density matrix of the excitation

evolves according to the formula

$$\hat{\rho}'(t+1) = \sum_{\mathcal{K}} p_{\mathcal{K}} \hat{U}_{\mathcal{K}} \hat{\rho}(t) \hat{U}_{\mathcal{K}}^{\dagger}, \quad (13)$$

where \mathcal{K} denotes the possible edge configuration, $p_{\mathcal{K}}$ is the probability of the configuration \mathcal{K} and $\hat{U}_{\mathcal{K}}$ is a quantum walk on a ring with edge configuration \mathcal{K} . The random unitary channel (13) is followed by the projection

$$\hat{\rho}(t+1) = \hat{\pi} \hat{\rho}'(t+1) \hat{\pi}^{\dagger}, \quad (14)$$

which corresponds to the action of the sink. For simplicity, we consider that every edge occurs with the same probability p independent of its position. The probability of the edge configuration \mathcal{K} is then given by

$$p_{\mathcal{K}} = p^{|\mathcal{K}|} (1-p)^{2N-|\mathcal{K}|},$$

where $|\mathcal{K}|$ denotes the size of the set \mathcal{K} , i.e. the number of edges present in that configuration. The evolution operator $\hat{U}_{\mathcal{K}}$ of the walk on a percolated ring with edge configuration \mathcal{K} has the form

$$\hat{U}_{\mathcal{K}} = \hat{S}_{\mathcal{K}} \cdot (\hat{I}_P \otimes \hat{C}),$$

where $\hat{S}_{\mathcal{K}}$ is the step operator on the percolated ring. If the edge between m and $m+1$ is broken then the jumps from m to $m+1$ and from $m+1$ to m cannot occur. Instead, the coin states corresponding to the jumps undergoes a reflection, i.e.

$$|m\rangle|R\rangle \rightarrow |m\rangle|L\rangle, \quad |m+1\rangle|L\rangle \rightarrow |m+1\rangle|R\rangle. \quad (15)$$

Hence, the step operator $\hat{S}_{\mathcal{K}}$ on the percolated ring is given by

$$\begin{aligned} \hat{S}_{\mathcal{K}} = & \sum_{(m,m+1) \in \mathcal{K}} |m\rangle\langle m+1| \otimes |L\rangle\langle L| + |m+1\rangle\langle m| \otimes |R\rangle\langle R| + \\ & + \sum_{(m,m+1) \notin \mathcal{K}} |m\rangle\langle m| \otimes |L\rangle\langle R| + |m+1\rangle\langle m+1| \otimes |R\rangle\langle L| + \\ & + \sum_m |m\rangle\langle m| \otimes |S\rangle\langle S|. \end{aligned}$$

The evolution of a dynamically percolated quantum walk is rather involved. Nevertheless, it simplifies considerably in the asymptotic regime where it is described by the attractors satisfying

$$\hat{U}_{\mathcal{K}} \hat{X} \hat{U}_{\mathcal{K}}^{\dagger} = \lambda \hat{X}, \quad \forall \mathcal{K}, \quad \text{with } |\lambda| = 1.$$

Moreover, substantial part of the attractor space is spanned by the so-called p-attractors [49, 50], which can be constructed from the common eigenstates of all $\hat{U}_{\mathcal{K}}$'s. The common eigenstate $|\xi\rangle$ has to satisfy the equations

$$\hat{U}_{\mathcal{K}} |\xi\rangle = \beta |\xi\rangle,$$

for all possible configurations \mathcal{K} . We search for the common eigenstates in the form

$$|\xi\rangle = \sum_m |m\rangle |\xi^m\rangle,$$

where the coin state at position m is given by

$$|\xi^m\rangle = \xi_L^m |L\rangle + \xi_S^m |S\rangle + \xi_R^m |R\rangle.$$

Following [49, 50] we find that the amplitudes of the common eigenstate have to fulfill the shift conditions

$$\xi_L^m = \xi_R^{m+1}, \quad \forall m. \quad (16)$$

Moreover, the common eigenstates have to fulfill the coin conditions

$$\hat{\mathcal{R}}\hat{\mathcal{C}}|\xi^m\rangle = \beta|\xi^m\rangle, \quad \forall m, \quad (17)$$

where $\hat{\mathcal{R}}$ is the reflection operator which performs the operation (15). In the standard basis of the coin space it is given by the matrix

$$\mathcal{R} = \begin{pmatrix} 0 & 0 & 1 \\ 0 & 1 & 0 \\ 1 & 0 & 0 \end{pmatrix}.$$

Let us now test when the stationary states of the non-percolated (ideal) walk satisfy the common eigenstates conditions. From (8) it follows that the amplitudes of the stationary state $|s_n\rangle$ are given by

$$\begin{aligned} \xi_L^m &= \delta_{m,n} \sqrt{1 - \rho^2}, \\ \xi_S^m &= (\delta_{m,n} + \delta_{m,n+1}) \frac{\rho}{\sqrt{2}}, \\ \xi_R^m &= \delta_{m,n+1} \sqrt{1 - \rho^2} e^{i\alpha}. \end{aligned}$$

Hence, we find that the shift conditions (16) are fulfilled only for $\alpha = 0$. One can check that the coin conditions (17) are also satisfied only in this case. Hence, for $\alpha = 0$ the percolations do not eliminate the stationary states (8) - they remain as common eigenstates of all $\hat{U}_{\mathcal{K}}$'s. Moreover, the stationary states $|s_n\rangle$ with $n \in \{-N+1, \dots, N-2\}$ are not affected by the projection $\hat{\pi}$ corresponding to the effect of the sink. Therefore, for $\alpha = 0$ the trapping effect is preserved in the percolated walk and the efficiency of transport to the sink is not improved, i.e. η depends on the initial coin state in the same way as for the ideal walk. On the other hand, for $\alpha \neq 0$ the stationary states (8) do not satisfy the common eigenstates conditions and they are sensitive to percolations. Hence, for $\alpha \neq 0$ dynamical percolations of the ring eliminate the trapping effect and the transport of excitation is efficient, i.e. $\eta = 1$ for all initial coin states. We see that percolations nullify the equivalence of coins with different values of α which holds for ideal walks.

For illustration we display in Figure 6 the survival probability for one random realization of dynamically percolated quantum walk. On the left we have chosen $\alpha = 0$,

for which the stationary states (8) are unaffected by percolations. We find that the survival probability levels at the same value as for the ideal walk (see the right plot of Figure 5 for comparison). The plot on the right shows the survival probability when $\alpha = \pi$. In this case percolations cancel the trapping effect and the survival probability decays exponentially.

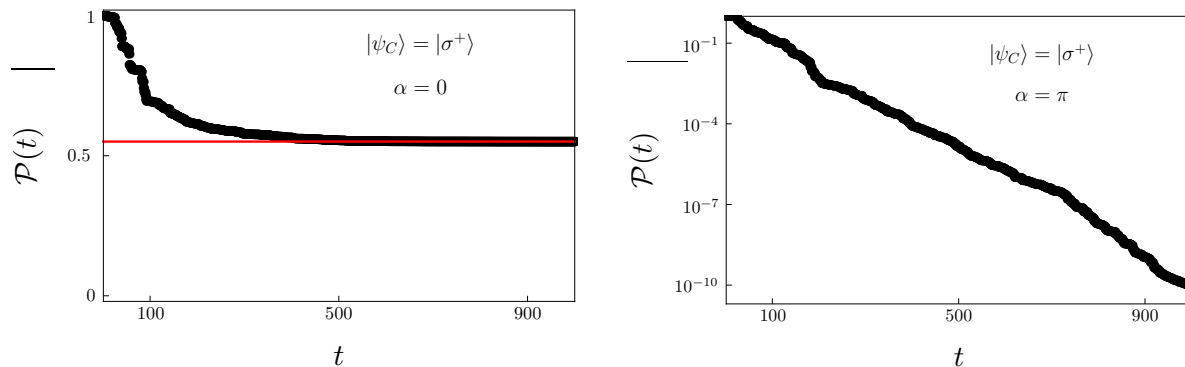


Figure 6. Survival probability for percolated quantum walk. The initial coin state was chosen as $|\sigma^+\rangle$. The probability of edge presence is $p = \frac{1}{2}$. On the left we have considered the phase $\alpha = 0$. In this case, percolations do not eliminate the trapping effect and the survival probability does not drop below the same value as for the non-percolated walk (see the right plot of Figure 5). On the other hand, for $\alpha = \pi$, which we display in the right plot, the trapping effect vanishes. The survival probability decreases exponentially, which we highlight with the log-scale. The deviations from the straight line stem from the fact that the plot corresponds to a single random realization of the percolated walk.

The decay rate γ of the survival probability depends on both parameters of the coin ρ and α and also on the probability of edge presence p . The numerical simulations indicate that the decay rate can be estimated according to

$$\gamma = 1 - |\lambda_l|, \quad (18)$$

where λ_l is the leading eigenvalue of the superoperator

$$\Phi = \sum_{\kappa} p_{\kappa} \left(\hat{\pi} \hat{U}_{\kappa} \right) \otimes \left(\hat{\pi} \hat{U}_{\kappa}^* \right), \quad (19)$$

which describes the evolution of the density matrix consisting of the random unitary channel (13) and the projection onto the sink (14). Compared to Eq. (2) the factor 2 is missing due to the use of the superoperator formalism. In (19) star denotes the complex conjugation.

For illustration we display in Figures 7, 8 and 9 the decay rate as a function of the phase α , coin parameter ρ and the edge presence probability p , respectively. The size of the ring is given by $N = 5$. The red curves are given by the formula (18) while the black dots are obtained from numerical simulation where we fit the exponential decay (1) to the survival probability averaged over 1000 random realizations of percolated quantum walk.

In Figure 7 we plot the decay rate as a function of the phase α while fixing the coin parameter $\rho = \frac{1}{\sqrt{3}}$ and the edge presence probability $p = \frac{1}{2}$. For small values of α the decay rate tends to zero, as can be expected. Notice that maximal decay rate is not obtained for $\alpha = \pi$, but rather for $\alpha \approx \frac{47}{50}\pi$. We have not found a simple explanation for this effect. The numerical simulations indicate that the position of the peak drifts further away from $\frac{\pi}{2}$, however, very mildly. For $\alpha \in (\pi, 2\pi)$ the plot would be the mirror image of the presented one.

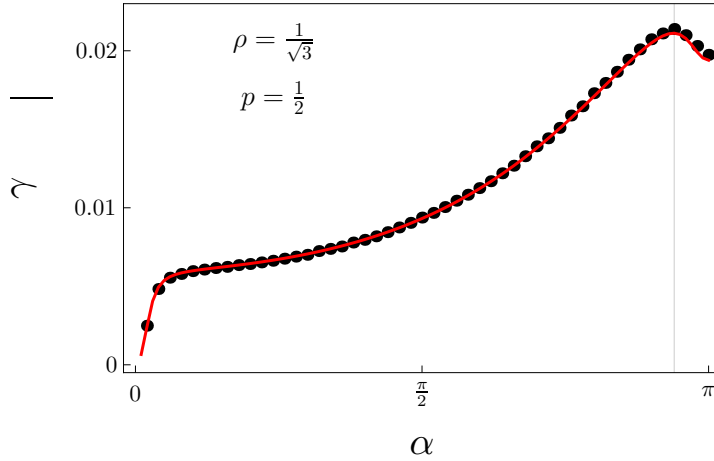


Figure 7. Decay rate as a function of the phase α . The other parameters have been chosen as $\rho = \frac{1}{\sqrt{3}}$ and $p = \frac{1}{2}$. The maximal decay rate is reached for $\alpha \approx \frac{47}{50}\pi$.

The decay rate in dependence on the coin parameter ρ is displayed in Figure 8. The remaining parameters were chosen as $p = \frac{1}{2}$ and $\alpha = \pi$.

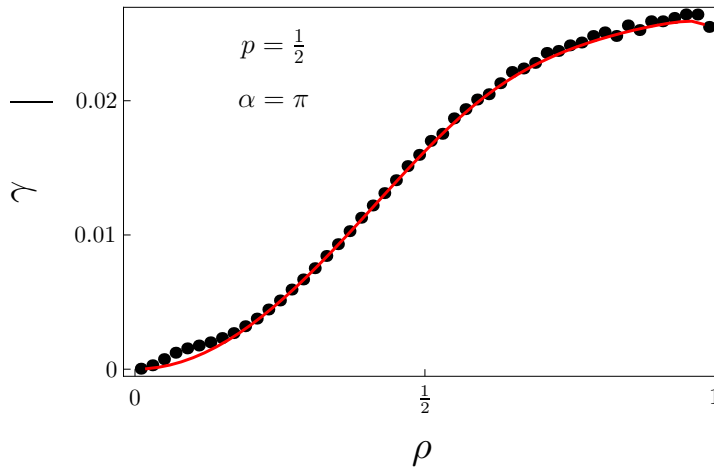


Figure 8. Decay rate as a function of the probability of the coin parameter ρ . We have considered $p = \frac{1}{2}$ and $\alpha = \pi$.

Figure 9 shows the decay rate as a function of the edge presence probability p for fixed $\rho = \frac{1}{\sqrt{3}}$ and $\alpha = \pi$. Notice the asymmetry of the curve. The maximal decay rate

is reached for $p \approx 0.55$. The numerical simulations indicate that with increasing N the position of the maximum tends to $p = 0.5$

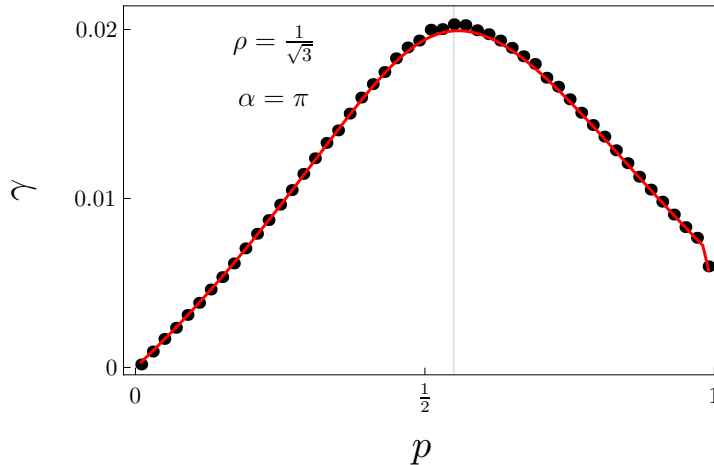


Figure 9. Decay rate as a function of the probability of edge presence probability p for fixed $\rho = \frac{1}{\sqrt{3}}$ and $\alpha = \pi$. The maximal decay rate is obtained for $p \approx 0.55$.

In summary, percolations eliminate the trapping effect provided that the coin parameter α is non-zero. This leads to exponential decay of the survival probability with the decay rate determined by the leading eigenvalue of the superoperator (19). However, for $\alpha = 0$ the trapping effect is robust to percolations and the transport efficiency is not improved.

6. Conclusions

We have analyzed the absorption problem for discrete-time quantum walks on a ring. Using both numerical as well analytic methods we determined several properties of this model of transport. For a two-state quantum walk the transport of excitation to the sink is efficient and the survival probability decays exponentially independent of the initial coin state. The decay rate is determined by the coin operator and the size of the ring. In this respect we completed the analysis presented previously.

Next, we have considered a two-parameter set of lazy quantum walk which exhibits the trapping effect. Compared to the two state quantum walk the lazy walk shows a much richer dynamics. Indeed, the survival probability has a non-vanishing lower bound and the excitation transport is inefficient, except for a particular initial coin state. We have determined the dependency of the transport efficiency on the initial coin state, the coin operator and the size of the ring.

Finally, we have shown that the trapping effect can be eliminated by dynamical percolations of the ring provided that the phase parameter α of the coin operator is non-zero. In such a case, the survival probability decays exponentially independent of the initial condition. The decay rate is determined by the parameters of the coin and

percolations. However, for $\check{\alpha} = 0$ the stationary states are resilient to percolations and the trapping effect is preserved. We note that in the framework of continuous-time quantum walks similar effects have been found in [51, 52, 53, 54].

The trapping effect is present also in quantum walks on more complicated graphs driven by higher dimensional coins. It would be interesting to find conditions under which it is robust under percolations, or, on the contrary, what type of percolation is sufficient to eliminate the trapping effect and allow for efficient transfer. In this way studies of percolated quantum walk could contribute to our understanding of transport along complicated molecular structures and ways how to control it.

Finally, let us briefly comment on the possible physical implementations of the lazy walk model. Since the model requires three internal states, usual optical implementations based on polarization are not applicable, at least not in a straightforward way. However, one may employ optical angular momentum [55] or interferometric multiports [56]. Additional candidates might be realizations of quantum walk in phase space [57, 58] or using trapped three-level atoms [59, 60].

Acknowledgments

We acknowledge the financial support from RVO 68407700. MŠ is grateful for the financial support from GAČR 14-02901P. IJ is grateful for the financial support from GAČR 13-33906S.

Appendix A. Survival probability for a two-state walk

In this appendix we show that the survival probability for a two-state quantum walk model which we have discussed in Section 3 is independent of the initial coin state. The key ingredients of the proof are the results of [34] and the fact that we consider a highly symmetric situation. Namely, the excitation enters the ring exactly opposite of the sink.

In [34] the authors have studied the absorption problem for a two-state quantum walk on a finite line with vertices $\{0, \dots, n\}$ with sinks on both ends 0 and n . In particular, they have focused on the probability $P_k^{(n)}(t, \psi_C)$ that the excitation starting the walk at the vertex k with the initial state $\psi_C = (\psi_L, \psi_R)^T$ is absorbed at the vertex 0 after t steps of the walk. By $\psi_{L,R}$ we have denoted the amplitudes of the initial coin state in the standard basis, i.e.

$$|\psi_C\rangle = \psi_L|L\rangle + \psi_R|R\rangle.$$

It is straightforward to see that the survival probability $\mathcal{P}(t)$ for the two-state walk on a ring of size $2N$ can be written equivalently as

$$\mathcal{P}(t) = 1 - \left(P_N^{(2N)}(t, \psi_C) + \tilde{P}_N^{(2N)}(t, \psi_C) \right), \quad (\text{A.1})$$

where we have denoted by $\tilde{P}_N^{(2N)}(t, \psi_C)$ the probability of absorption at the vertex $2N$. We now prove that the sum $P_N^{(2N)}(t, \psi_C) + \tilde{P}_N^{(2N)}(t, \psi_C)$ is independent of the initial coin

state ψ_C . It was shown in [34] that the probability of absorption at 0 can be expressed in the form

$$P_N^{(2N)}(t, \psi_C) = C_1(t)|\psi_L|^2 + C_2(t)|\psi_R|^2 + 2\text{Re}(C_3(t)\psi_L^*\psi_R). \quad (\text{A.2})$$

The coefficients $C_i(t)$ are determined by the coin operator. For the choice of the coin (4) they read

$$\begin{aligned} C_1(t) &= \left| \rho p_N^{(2N)}(t) + \sqrt{1 - \rho^2} r_N^{(2N)}(t) \right|^2, \\ C_2(t) &= \left| \sqrt{1 - \rho^2} p_N^{(2N)}(t) - \rho r_N^{(2N)}(t) \right|^2, \\ C_3(t) &= \left(\rho p_N^{(2N)}(t) + \sqrt{1 - \rho^2} r_N^{(2N)}(t) \right)^* \left(\sqrt{1 - \rho^2} p_N^{(2N)}(t) - \rho r_N^{(2N)}(t) \right). \end{aligned}$$

The quantities $p_N^{(2N)}(t)$ and $r_N^{(2N)}(t)$ were analyzed in [34]. They also depend on the coin operator and for the choice of the coin (4) they are real valued. Hence, we can omit the complex conjugation in the formula for $C_3(t)$ since all terms involved are real.

Let us now turn to the probability of absorption at the vertex $2N$. This was not considered in [34], however, it is straightforward to map it to the probability of absorption at the vertex 0. Indeed, by interchanging the coin states $|L\rangle$ and $|R\rangle$ we can express $\tilde{P}_N^{(2N)}(t, \psi_C)$ as the probability of absorption at 0 in a quantum walk with the coin operator

$$\tilde{C}^{(2)} = \begin{pmatrix} -\rho & \sqrt{1 - \rho^2} \\ \sqrt{1 - \rho^2} & \rho \end{pmatrix},$$

starting with the initial coin state

$$|\tilde{\psi}_C\rangle = \psi_R|L\rangle + \psi_L|R\rangle.$$

Here we also use the symmetry of the problem, i.e. the fact that the distance from the starting point of the walk to sinks at 0 and $2N$ is the same. Modifying the formula (A.2) accordingly we find that the probability of absorption at the vertex $2N$ reads

$$\tilde{P}_N^{(2N)}(t, \psi_C) = \tilde{C}_1(t)|\psi_R|^2 + \tilde{C}_2(t)|\psi_L|^2 + 2\text{Re}\left(\tilde{C}_3(t)\psi_L\psi_R^*\right),$$

with coefficients $\tilde{C}_i(t)$ given by

$$\begin{aligned} \tilde{C}_1(t) &= \left| -\rho \tilde{p}_N^{(2N)}(t) + \sqrt{1 - \rho^2} \tilde{r}_N^{(2N)}(t) \right|^2, \\ \tilde{C}_2(t) &= \left| \sqrt{1 - \rho^2} \tilde{p}_N^{(2N)}(t) + \rho \tilde{r}_N^{(2N)}(t) \right|^2, \\ \tilde{C}_3(t) &= \left(-\rho \tilde{p}_N^{(2N)}(t) + \sqrt{1 - \rho^2} \tilde{r}_N^{(2N)}(t) \right) \left(\sqrt{1 - \rho^2} \tilde{p}_N^{(2N)}(t) + \rho \tilde{r}_N^{(2N)}(t) \right). \end{aligned}$$

Following [34] we find that the quantities $\tilde{p}_N^{(2N)}(t), \tilde{r}_N^{(2N)}(t)$ are related to $p_N^{(2N)}(t), r_N^{(2N)}(t)$ through the formula

$$\begin{aligned} \tilde{p}_N^{(2N)}(t) &= (-1)^{N-1} p_N^{(2N)}(t), \\ \tilde{r}_N^{(2N)}(t) &= (-1)^N r_N^{(2N)}(t). \end{aligned}$$

It is then straightforward to show that

$$\begin{aligned}\tilde{C}_1(t) &= C_1(t), \\ \tilde{C}_2(t) &= C_2(t), \\ \tilde{C}_3(t) &= -C_3(t).\end{aligned}$$

Hence, the sum of the probabilities of absorption at vertices 0 and $2N$ reads

$$\begin{aligned}P_N^{(2N)}(t, \psi_C) + \tilde{P}_N^{(2N)}(t, \psi_C) &= C_1(t) + C_2(t) + \\ &+ 2\text{Re}(C_3(t) (\psi_L^* \psi_R - \psi_L \psi_R^*)),\end{aligned}\quad (\text{A.3})$$

where we have used the normalization condition of the initial coin state

$$|\psi_L|^2 + |\psi_R|^2 = 1.$$

Moreover, since $C_3(t)$ is real and $\psi_L^* \psi_R - \psi_L \psi_R^*$ is purely imaginary the last term in (A.3) vanishes. Hence, we find that (A.3) is independent of the initial coin state and through the relation (A.1) the same holds for the survival probability $\mathcal{P}(t)$. This completes our proof.

References

- [1] Aharonov Y, Davidovich L and Zagury N 1993 *Phys. Rev. A* **48** 1687
- [2] Meyer D 1996 *J. Stat. Phys.* **85** 551
- [3] Farhi E and Gutmann S 1998 *Phys. Rev. A* **58** 915
- [4] Shenvi N, Kempe J and Whaley K 2003 *Phys. Rev. A* **67** 052307
- [5] Childs A M and Goldstone J 2004 *Phys. Rev. A* **70** 022314
- [6] Reitzner D, Hiller M, Feldman E and Bužek V 2009 *Phys. Rev. A* **79** 012323
- [7] Potoček V, Gabris A, Kiss T and Jex I 2009 *Phys. Rev. A* **79** 012325
- [8] Childs A M and Ge T 2014 *Phys. Rev. A* **89** 052337
- [9] Kendon V M and Tamon C 2011 *J. Comput. Theor. Nanosc.* **8** 422
- [10] Kurzynski P and Wojcik A 2011 *Phys. Rev. A* **83** 062315
- [11] Barr K E, Proctor T J, Allen D and Kendon V M 2014 *Quantum Inf. Comput.* **14** 417
- [12] Zhan X, Qin H, Bian Z H, Li J and Xue P 2014 *Phys. Rev. A* **90** 012331
- [13] Yalcinkaya I and Gedik Z 2015 *J. Phys. A* **48** 225302
- [14] Gamble J K, Friesen M, Zhou D, Joynt R and Coppersmith S N 2010 *Phys. Rev. A* **81** 052313
- [15] Berry S D and Wang J B 2011 *Phys. Rev. A* **83** 042317
- [16] Rudinger K, Gamble J K, Wellons M, Bach E, Friesen M, Joynt R and Coppersmith S N 2012 *Phys. Rev. A* **86** 022334
- [17] Hillery M, Reitzner D and Bužek V 2010 *Phys. Rev. A* **81** 062324
- [18] Hillery M, Zheng H J, Feldman E, Reitzner D and Bužek V 2012 *Phys. Rev. A* **85** 062325
- [19] Cottrell S and Hillery M 2014 *Phys. Rev. Lett.* **112** 030501
- [20] Childs A M 2009 *Phys. Rev. Lett.* **102** 180501
- [21] Lovett N B, Cooper S, Everitt M, Trevers M and Kendon V 2010 *Phys. Rev. A* **81** 042330
- [22] Karski M, Förster L, Choi J, Steffen A, Alt W, Meschede D and Widera A 2009 *Science* **325** 174
- [23] Schmitz H, Matjeschk R, Schneider C, Glueckert J, Enderlein M, Huber T and Schaetz T 2009 *Phys. Rev. Lett.* **103** 090504
- [24] Zähringer F, Kirchmair G, Gerritsma R, Solano E, Blatt R and Roos C F 2010 *Phys. Rev. Lett.* **104** 100503
- [25] Schreiber A, Cassemiro K N, Potoček V, Gábris A, Mosley P J, Andersson E, Jex I and Silberhorn C 2010 *Phys. Rev. Lett.* **104** 050502

- [26] Broome M A, Fedrizzi A, Lanyon B P, Kassal I, Aspuru-Guzik A and White A G 2010 *Phys. Rev. Lett.* **104** 153602
- [27] Peruzzo A, Lobino M, Matthews J C F, Matsuda N, Politi A, Poulios K, Zhou X, Lahini Y, Ismail N, Wörhoff K, Bromberg Y, Silberberg Y, Thompson M G and O'Brien J L 2010 *Science* **3329** 1500
- [28] Owens J O, Broome M A, Biggerstaff D N, Goggin M E, Fedrizzi A, Linjordet T, Ams M, Marshall G D, Twamley J, Withford M J and White A G 2011 *New J. Phys.* **13** 075003
- [29] Sansoni L, Sciarrino F, Vallone G, Mataloni P, Crespi A, Ramponi R and Osellame R 2012 *Phys. Rev. Lett.* **108** 010502
- [30] Schreiber A, Gábris A, Rohde P P, Laiho K, Štefaňák M, Potoček V, Hamilton C, Jex I and Silberhorn C 2012 *Science* **336** 55
- [31] Jeong Y C, Di Franco C, Lim H T, Kim M S and Kim Y H 2013 *Nature Comm.* **4** 2471
- [32] Elster F, Barkhofen S, Nitsche T, Novotný J, Gábris A, Jex I and Silberhorn C 2015 *Sci. Rep.* **5** 13495
- [33] Ambainis A, Bach E, Nayak A, Vishwanath A and Watrous J 2001 in *Proceedings of the Thirty-Third Annual ACM Symposium on Theory of Computing* 37
- [34] Konno N, Namiki T, Soshi T and Sudbury A 2003 *J. Phys. A* **36** 241
- [35] Bach E, Coppersmith S, Goldschén M P, Joynt R and Watrous J 2004 *J. Comput. System Sci.* **69** 562
- [36] Yamasaki T, Kobayashi H and Imai H 2003 *Phys. Rev. A* **68** 012302
- [37] Kwek L C and Setiawan 2011 *Phys. Rev. A* **84** 032319
- [38] Chandrashekar C M and Busch T 2014 *Quantum Inf. Proc.* **13** 1313
- [39] Asboth J K and Edge J M 2015 *Phys. Rev. A* **91** 022324
- [40] Inui N, Konno N and Segawa E 2005 *Phys. Rev. E* **72** 056112
- [41] Inui N and Konno N 2005 *Physica A* **353** 133
- [42] Štefaňák M, Bezděková I and Jex I 2012 *Eur. Phys. J. D* **66** 142
- [43] Štefaňák M, Bezděková I, Jex I and Barnett S M 2014 *Quantum Inf. Comput.* **14** 1213
- [44] Grimmett G 1999 *Percolation, Die Grundlehren der mathematischen Wissenschaften in Einzeldarstellungen* (Springer, New York)
- [45] Leung G, Knott P, Bailey J and Kendon V 2010 *New J. Phys.* **12** 123018
- [46] Goyal S K, Konrad T and Diosi L 2015 *Phys. Lett. A* **379** 100
- [47] Kempf A and Portugal R 2009 *Phys. Rev. A* **79** 052317
- [48] Štefaňák M, Bezděková I and Jex I 2014 *Phys. Rev. A* **90** 012342
- [49] Kollár B, Kiss T, Novotný J and Jex I 2012 *Phys. Rev. Lett.* **108** 230505
- [50] Kollár B, Novotný J, Kiss T, and Jex I 2014 *Eur. Phys. J. Plus* **129** 103
- [51] Muelken O and Blumen A 2011 *Phys. Rep.* **502** 37
- [52] Schijven P, Kohlberger J, Blumen A and Muelken O 2012 *J. Phys. A* **45** 215003
- [53] Anishchenko A, Blumen A and Muelken O 2013 *Phys. Rev. E* **88** 062126
- [54] Darázs Z, Anishchenko A, Kiss T, Blumen A and Muelken O 2014 *Phys. Rev. E* **90** 032113
- [55] Hamilton C S, Gábris A, Jex I and Barnett S M 2011 *New J. Phys.* **13** 013015
- [56] Hillery M, Bergou J A and Feldman E 2003 *Phys. Rev. A* **68** 032314
- [57] Xue P, Sanders B C, Blais A and Lalumiere K 2008 *Phys. Rev. A* **78** 042334
- [58] Xue P and Sanders B C 2008 *New J. Phys.* **10** 053025
- [59] Eckert K, Mompert J, Corbalan R, Lewenstein M and Birkl G 2006 *Optics Commun.* **264** 264
- [60] Sevincli S et al. 2011 *J. Phys. B* **44** 184018